11th World Congress on Computational Mechanics (WCCM XI)
5th European Conference on Computational Mechanics (ECCM V)
6th European Conference on Computational Fluid Dynamics (ECFD VI)
E. Oñate, J. Oliver and A. Huerta (Eds)

CORRELATION BASED INLET BOUNDARY CONDITIONS FOR IMPROVED TURBULENCE AND TRANSITION PREDICTION IN TURBOMACHINERY FLOWS

Christoph Bode[†], Thorben Aufderheide[†], Dragan Kožulović[‡] and Jens Friedrichs[†]

[†] Technische Universität Braunschweig, Institute of Jet Propulsion and Turbomachinery, Hermann-Blenk-Str. 37, D-38108 Braunschweig Germany, chr.bode@ifas.tu-bs.de

[‡] Hamburg University of Applied Sciences, Fakultät Technik und Informatik, Department Fahrzeugtechnik und Flugzeugbau, Berliner Tor 9, D-20099 Hamburg, Germany

Key words: RANS, Turbomachinery, Laminar-Turbulent Boundary-Layer Transition, Turbulent Length Scale.

Abstract. A correlation based approach for estimation of the turbulence length scale l_T at the inflow boundary is proposed and presented. This estimation yields reasonable turbulence decay, supporting the transition model in accurately predicting the laminar-turbulent transition location and development. As an additional element of the approach, the sensitivity of the turbulence model to free stream values is suppressed by limiting the eddy viscosity in non-viscous regions. Therefore a criterion to detect those regions, based only on local variables, is derived. The method is implemented in DLR's turbomachinery flow solver TRACE in the framework of the $k-\omega$ turbulence model by Wilcox 1988 [1] and the $\gamma - Re_\theta$ transition model by Langtry and Menter [2]. The improved model is tested to the T161 turbine test case [3] and validated at the ERCOFTAC T3X flat plate [4], U-Duct by Monson & Seegmiller [5] and Curved-Bend by So & Mellor [6].

1 INTRODUCTION

Laminar-turbulent transition plays a significant role in the boundary layer development of modern highly-loaded low-pressure turbine (LPT) profiles, and to a smaller degree for compressor profiles. The significance is even accentuated due to the drop of Reynolds numbers at high flight altitudes, that means at cruise conditions. Some turbine profiles operate at Reynolds numbers as low as $Re_{2th} \leq 1.0 \cdot 10^5$, showing a large laminar boundary layer patch with subsequent separation and turbulent reattachment. There exist many approaches for the prediction of laminar-turbulent transition. For turbomachinery flows, a combination of a RANS turbulence model with a correlation-based transition model is widely spread. In this work, the combination of the k-ω turbulence model by Wilcox 1988 [1] and the γ-Re_θ transition model by Langtry and Menter [2] is applied. In the present framework, the influence of the turbulence length scale (l_T) on the turbulence decay behaviour of the turbulence model is investigated. Depending on the prescribed turbulence length scale at the inflow boundary, different dissipation rates will arise, with significantly altered decay of turbulence intensity. This leads to a shift in transition prediction, since the transition model is coupled to the turbulence intensity, cf. for example Bode et al. [7] [8] and Moore and Moore [9]. Turbomachinery flows are very prone to this effect, due to high turbulence levels and corresponding sensitivity to dissipation rate (or length scale) prescription. As many experiments do not provide the turbulence length scale, the CFD users feel free to choose a value, often one that best fits the experimental data. Hence, a correlation for the estimation of the turbulence length scale is derived. This correlation reasonably fits various experimental data.

2 COMPUTATIONAL METHOD

2.1 TRACE Code

An up-to-date numerical method, the parallel CFD-solver TRACE of DLR Cologne has been applied. In this paper the turbulence is modelled by the two-equation $k-\omega$ model of Wilcox 1988 [1], together with the Kato-Launder [10] fix for the stagnation point anomaly. To capture the streamline curvature effects the $k-\omega$ turbulence model has been modified using local variables only, cf. Kožulović [11]. The boundary layer transition has been modelled by the two-equation $\gamma - Re_\theta$ model of Langtry and Menter [2]. For a more detailed description of the model see Langtry and Menter [2] and for detailed information about the used CFD setup see Bode et al. [8].

2.2 Approach Description and Testing

The new viscous blending (VB) approach has been tested and validated for three different low pressure turbine (LPT) cascades in Bode et al. [8]. Nevertheless the effect of the turbulence length scale on turbulence and transition prediction is shown here in detail for the T161 turbine cascade. In this paper different prescribed turbulence length scales (Sim. l_T=$10^{-2} - 10^{-5}$m) togehther with the new viscous blending approach (VB) are shown and compared to new experimental results, at low speed conditions to validate the new approach (VB). The applied grid consist of 923.648 nodes and is shown in figure 1 a). Besides figure 1 a), where the geometry and some streamwise positions are marked, figure 1 b) gives an idea of the measuring planes which are used for this test case. Today linear eddy viscosity models are the workhorse for aerospace engineers. Those linear models use the Boussinesq assumption to get the relationship between the mean strain rate and the Reynolds stress tensor, cf. equation 1.

$$\tau_{T,ij} = -\overline{\rho u_i'' u_j''} = 2\mu_T s_{ij} - \frac{2}{3}\rho k \delta_{ij} \tag{1}$$

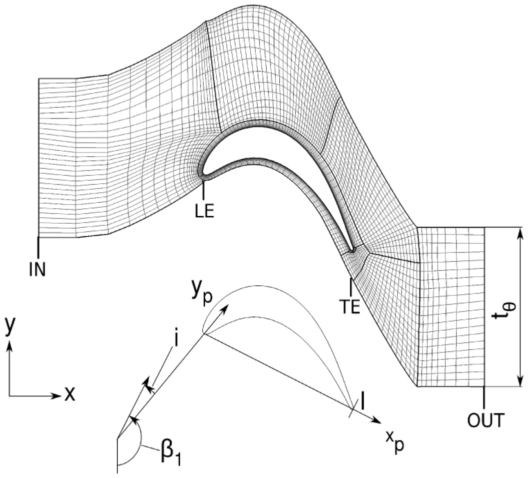

(a) Computational Domain T161

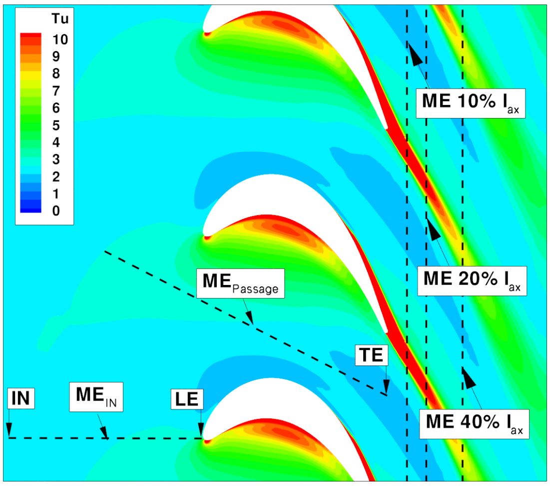

(b) Measuring Plane (ME) Definitions for T161

Figure 1: T161 Turbine Cascade Test Case

This equation 1 is reduced to the closure problem of the scalar eddy viscosity μ_T. The main task of turbulence modelling is to get a relationship between turbulent quantities such as turbulent kinetic energy k, turbulent dissipation rate ω and eddy viscosity μ_T. For the $k-\omega$ two-equation turbulence modell after Wilcox 1988 [1] the eddy viscosity is determined as follows

$$\mu_T = C_\mu \frac{\rho k}{\omega}, \tag{2}$$

with $C_\mu = 1$, as used in many applications. In Turbomachinery flow, especially in turbine and compressor cascades with high turbulence intensity and moderate turbulent decay rates, this approach will result in too high loss prediction. As a result the CFD-user changes the turbulent length scale and hence the turbulent decay rate (because this is often missing in the experiments) to best fit the experimental data. There exist several rules of thumb or best practice guides for the prescription of the turbulent length scale, which usually lead to $l_T \approx 10^{-4} m$ for typical turbomachinery conditions. But, this leads to extremely harsh turbulent decay rates which implies incorrect values of turbulent levels and this finally results in a wrong prediction of transitional behaviour on turbomachinery blades. In this new approach (VB) both inaccuracies will be eliminated.

Inlet Boundary Dissipation Rate / Turbulent Length Scale In TRACE the free stream dissipation rate at the inlet boundary is computed as follows

$$\omega_{FS} = \frac{\sqrt{k}}{l_T} \tag{3}$$

and needs therefore l_T from the CFD-user, see above. Here, an estimation is derived in the style of the correlation of Baines and Peterson [12]. Originally, this correlation applied to high turbulence flows through screens and reads as follows:

$$Tu = 1.12 \left(\frac{x}{b}\right)^{-\frac{5}{7}} \tag{4}$$

To get the information about the turbulent kinetic energy decay (dissipation rate at the

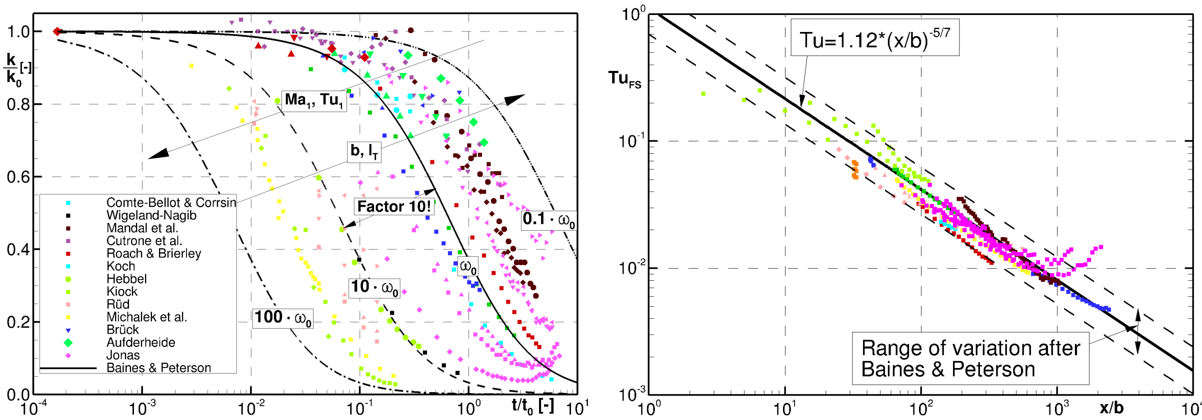

(a) Normalized Turbulent Kinetic Energy k/k0 (b) Free stream Turbulence Intensity Decay Tu$_{FS}$

Figure 2: Turbulence decay for several experiments

inlet boundary ω_{FS}) the solution of the destruction term of the k-equation after Wilcox [1] is needed and given by the following equation

$$\frac{k\,(t)}{k_0} = (\beta_\omega \omega_0 t + 1)^{-\frac{\beta_k}{\beta_\omega}} \tag{5}$$

with $\beta_k = 0.09$, $\beta_\omega = 0.075$ and k_0 as the value at the first measurement position. Herein the dissipation rate ω_0, at the inlet boundary, is derived to match the T3X flat plate testseries [4] to $\omega_0 = 220\ 1/s$, cf. Bode et al. [7]. Hence equation 5 can be rewritten as

$$\frac{k\,(t/t_0)}{k_0} = \left[\left(\frac{t}{t_0}\right) + 1\right]^{-1.2} \tag{6}$$

with $t_0 = 1/\left(\beta_\omega \cdot F \cdot \omega_0\right) = 0.0606s$ ($F = 1$ in this case). Now in figure 2 a) experimental data for the normalized turbulent kinetic energy decay $\frac{k}{k_0}$ from several experiments is shown. It is well seen that the correlation given by Baines and Peterson [12] after equation 6 (solid line) reflects only the experimental data for the T3X ERCOFTAC test cases [4] in a well appropriate way as described before. But the correlation differs for the other test cases by a factor F (dashed and dash-dotted lines). It is well known from the literature that the design of the turbulence generating grid and the test case conditions like Mach number Ma_1 and turbulence intensity Tu_1 strongly affect the decay behaviour. With this in mind the new correlation resulting from figure 2 a) is

$$\omega_{FS} = F \cdot \omega_0 = (69.73 \cdot (Ma_1 \cdot Tu_1)^{0.62} \cdot \omega_0). \tag{7}$$

The new turbulent dissipation rate is now computed from the information about inlet velocity (in this case Mach number) and inlet turbulence intensity. The design of the turbulence generating grid is not considered here. In figure 2 b) the same experimental data is shown for the free stream turbulence intensity (Tu_{FS}) dependent on the normalized distance from the turbulence generating grid (x/b), where b is the grid bar or rod diameter. The information from figure 2 b) is the good agreement of all experimental results, including the inhouse experiments, with the theory after Baines and Peterson. Also provides figure 2 b) confidence in the grid design and experimental measurement technique. Figure 3 shows a comparison of experimental data and numerical simulations

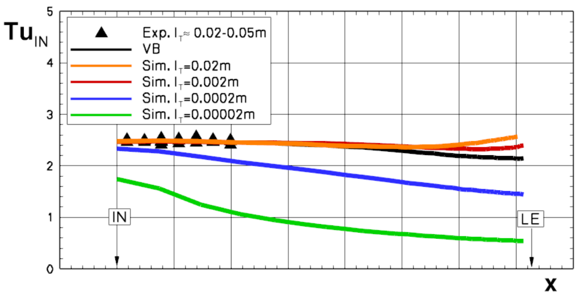

(a) Turbulence Intensity Decay At Inlet Tu$_{IN}$

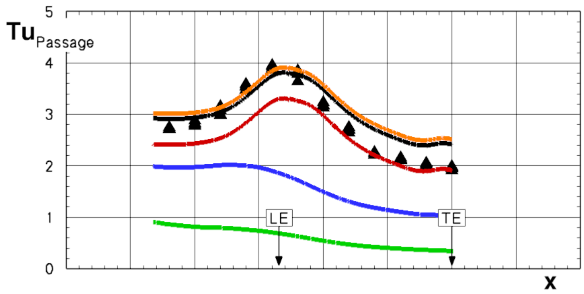

(b) Turbulence Intensity Behaviour At Passage Tu$_{Passage}$

Figure 3: Turbulence Intensity for T161 Turbine Cascade

with the new approach (VB using eqn. 7) and numerical simulations with different prescribed length scales (Sim. $l_T = 0.02m$ etc. using eqn. 3). In figure 3 a) the turbulence intensity decay from the inlet boundary to the leading edge ist shown. Figure 3 b) shows also the turbulence intensity behaviour but as figure 2 b) indicates in the passage of the turbine cascade. It is well seen that only, besides the new approach (VB), the numerical simulations with a prescribed turbulence length scale of $l_T = 0.02m$ and $l_T = 0.002m$ reflects the experimental data correctly. The other turbulence length scales results in a to strong decay of the turbulence intensity for both the inlet and passage flow.

Adaption of the Eddy Viscosity With the now correct prescription of the turbulent length scale (VB) the turbulent decay of the turbulence intensity results, after equation 2 with $C_\mu = 1$, in excessive high eddy viscosity because of the smaller decrease of the turbulent intensity and hence the higher amount of turbulent kinetic energy. There exist some approaches in the literature regarding a variable C_μ, cf. Durbin [13], Wilcox [1] and Menter [14] to name the most important. In this paper an approach is presented where the eddy viscosity from equation (2) is modified like Durbins time-scale bound, proposed in [13], where he predicts the eddy viscosity by

$$\mu_T = \frac{\rho k}{max\left(\omega, \frac{\sqrt{6}S}{\alpha}\right)} \tag{8}$$

or Menters implementation of the Bradshaw assumption [14] by

$$\mu_T = \frac{\rho a_1 k}{max\left(a_1\omega, F_2\Omega\right)}. \tag{9}$$

The testing of the Durbin approach, presented in Bode et al. [8], showed an unphysical behaviour of the eddy viscosity. Therefore the eddy viscosity after equation 8 and equation 9 is modified, so that the correct behaviour regarding overall characteristics and boundary layer development is given but the unphysical behaviour of the eddy viscosity is reduced. Also the use of the wall distance like in F_2 for Menters shear stress transport (SST) is avoided. For this reason, a criterion for the determination of viscous regions (boundary layers and wakes) has been developed as an additional element of the implemented approach (cf. [7] and [8]). This criterion is based on the large values of turbulent dissipation rate ω. It takes the relationship between the turbulent dissipation rate estimated from the $k-\omega$ turbulence model and the turbulent dissipation rate in the free stream of the flow estimated by the new approach after equation 7. The effect of the very high ratio in the boundary layer and wakes is used to separate them from the free stream. The derived reasonable range varies within the test cases. A good compromis is found for $0.0 \leq \frac{\omega}{\omega_{FS}} \leq 500$. The new variable $1/C_\mu =: b_v$ is shown in figure 4.

$$b_v = min\left[max\left[\left(\frac{\omega}{\omega_{FS}}\right), 0.1\right], 1.0\right]. \tag{10}$$

This leads to the new formulation of the eddy viscosity:

$$\mu_T = \frac{\rho a_1 k}{max\left(a_1\omega, b_v S\right)}. \tag{11}$$

As a result figure 5 a) shows the surface pressure distribution for numerical simulations with the new approach (VB using eqn. 7 and 11) and different prescribed l_T (using eqn. 3 and 2) compared to experimental data. The numerical results with the correct prescribed l_T from figure 3 results in a wrong surface pressure distribution with a fully turbulent boundary layer as figure 5 b) indicates. Here the smaller l_T show a correct boundary

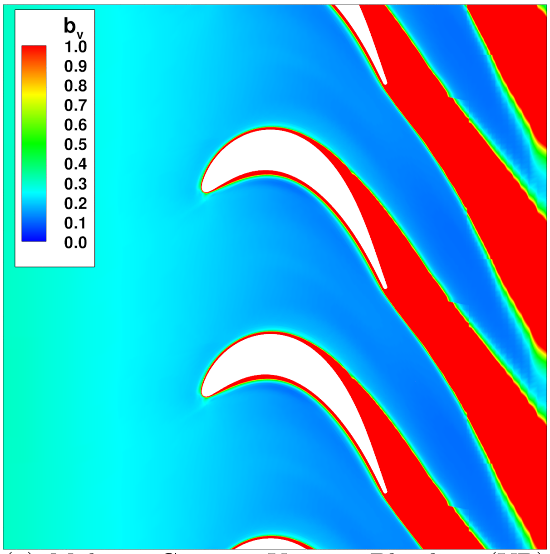

(a) Midspan-Contour Viscous Blending (VB) Variable b_v

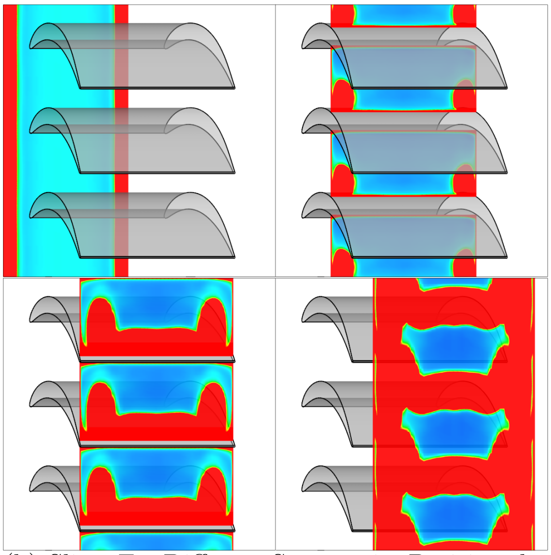

(b) Slices For Different Streamwise Positions b_v

Figure 4: New Criterion for the Determination of Viscous Regions for Computing Eddy Viscosity with the New Approach (VB)

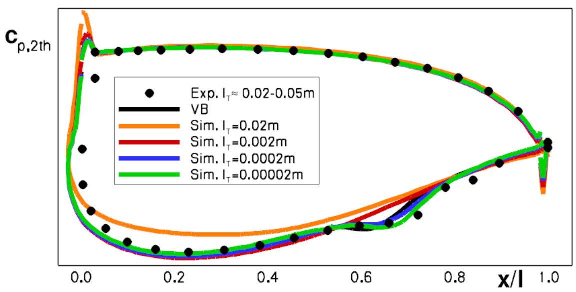

(a) Surface Pressure Coefficient c_p

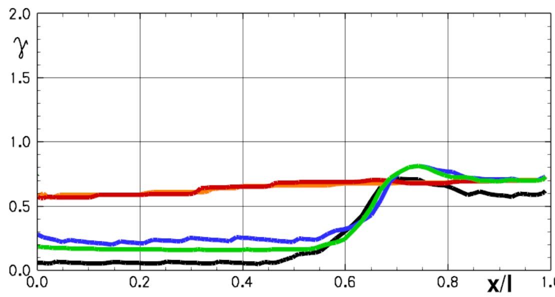

(b) Numerical Predicted Intermittency γ

Figure 5: Experimental and Numerical Boundary Layer Behaviour for the T161 Turbine Cascade

layer behaviour compared to the experiments. Also the simulation with the new approach (VB) is able to reproduce the surface pressure. Figure 6 shows a comparison of experimental and numerical results for the wake plane at the measuring plane ME 40%l_{ax}. Figure 6 a) shows the total pressure loss coefficient where figure 6 b) shows the turbulence intensity. Both figures indicates that a prescribed $l_T = 0.02m$ results in to high predicted total pressure loss due to the overproduction of turbulent kinetic energy (turbulent intensity) mainly on the suction surface (SS). The prescribed turbulence length scales in the range of $l_T = 0.002 - 0.00002m$ result in an adequat prediction of total pressure loss and

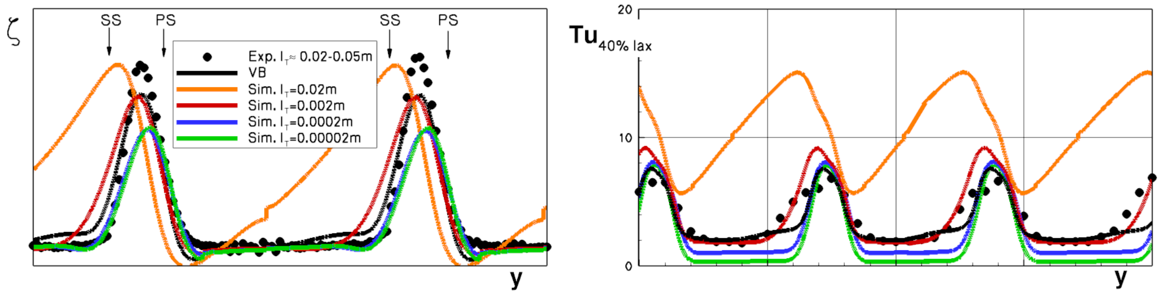

(a) Total Pressure Loss Coefficient ζ (b) Turbulence Intensity $\mathrm{Tu}_{ME40\%l_{ax}}$

Figure 6: Wake Traverse Measurements and Numerical Simulations at $ME = 40\%l_{ax}$ for the T161 Turbine Cascade

turbulence intensity in the wake plane, where the new approach (VB) is able to predict the transitional behaviour and the turbulence intensity decay best compared to the experiments. A closer look at figure 6 shows that the total pressure loss peaks and widths are better predicted and the mean levels of the turbulence intensity is best predicted by the new approach (VB).

3 VALIDATION OF THE NEW APPROACH (VB) WITH GENERIC TEST CASES

The remaining part of this paper will show the accuracy of the new approach (VB) by presenting test cases that have been computed with the TRACE solver and the new approach (VB) described in the previous section. As test cases 2D flat plate, curved bend and U-duct are presented.

3.1 ERCOFTAC T3X Flat Plate

To evaluate the new approach (VB) experiments on flat plates from Roach and Brierley [4] are compared to numerical simulations predicted with the new approach (VB). Contrary to the most numerical investigations, where k_{IN} and ω_{IN} must be prescribed at the computational inlet domain, here only the experimental information about the free stream turbulence intensity is directly prescribed at the inlet. With the information about the Mach number which is also provided in the experiments k_{IN} and ω_{IN} are computed after equation 7. Figure 7 a) indicates that equation 7 gives the correct decay behaviour of the turbulence intensity and no information about the turbulence length scale or dissipation rate is necessary. Figure 7 c)-f) shows that the transitional behaviour of all three flat plates is reproduced in an adequat manner by the new approach (VB). May the transition for the T3B is a little to early and the momentum thickness Reynolds number and the boundary layer thickness is somewhat underpredicted for all cases. Also the shape factor H_{12} in figure 7 f) indicates an earlyer transition for T3AM than the

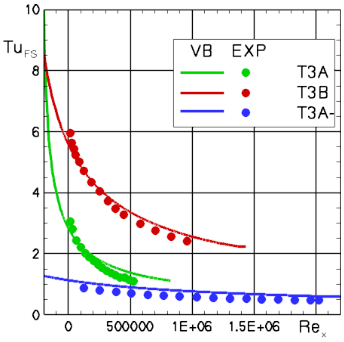

(a) Turbulence Intensity Tu$_{FS}$

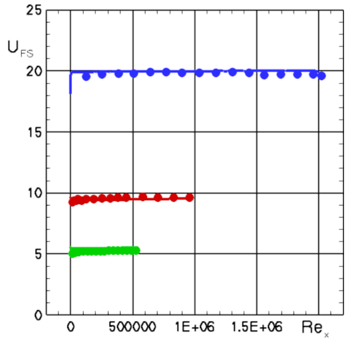

(b) Free stream Velocity U$_{FS}$

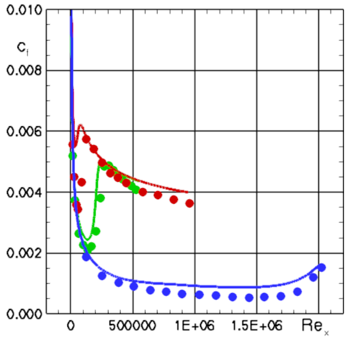

(c) Skin Friction Coefficient c$_f$

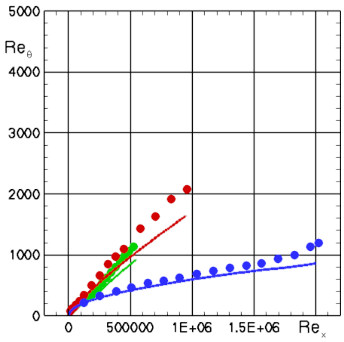

(d) Re$_\Theta$

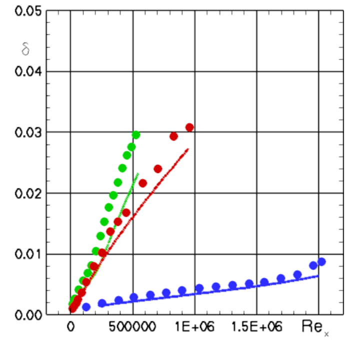

(e) Boundary Layer Thickness δ

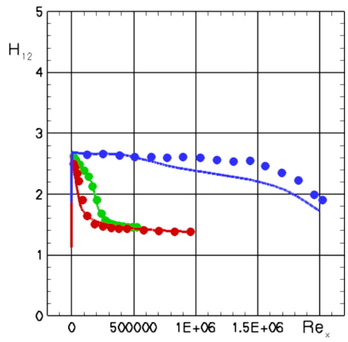

(f) Shape Factor H$_{12}$

Figure 7: Boundary Layer Values for T3X Flat Plate

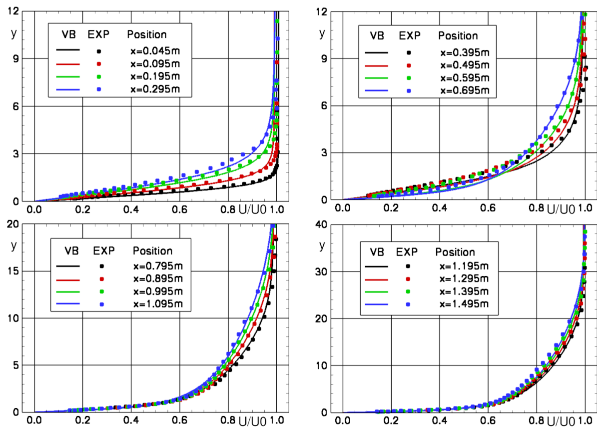

(a) Velocity Profiles U/U0

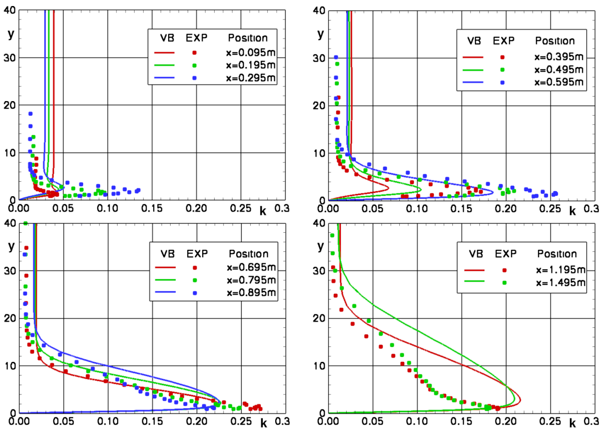

(b) Turbulent Kinetic Energy Profiles k

Figure 8: Boundary Layer Behaviour for T3A Flat Plate

experiments but the comparison of the skin friction coefficient in figure 7 c) is very good. In figure 8 a) the boundary layer velocity profiles U/U0 and in figure 8 b) the turbulent kinetic energy profiles k, for different streamwise positions, for the T3A flat plate are given. The comparison for the velocity profiles is very good. The turbulent kinetic energy profiles are not that good predicted but the trend and level of each profile is adequat.

3.2 Curved Bend And U-Duct

The curved bend test case of So and Mellor deals with the stabilizing (damping) effect of the surface curvature. Fig. 9 a) shows the geometry and the computational domain. The

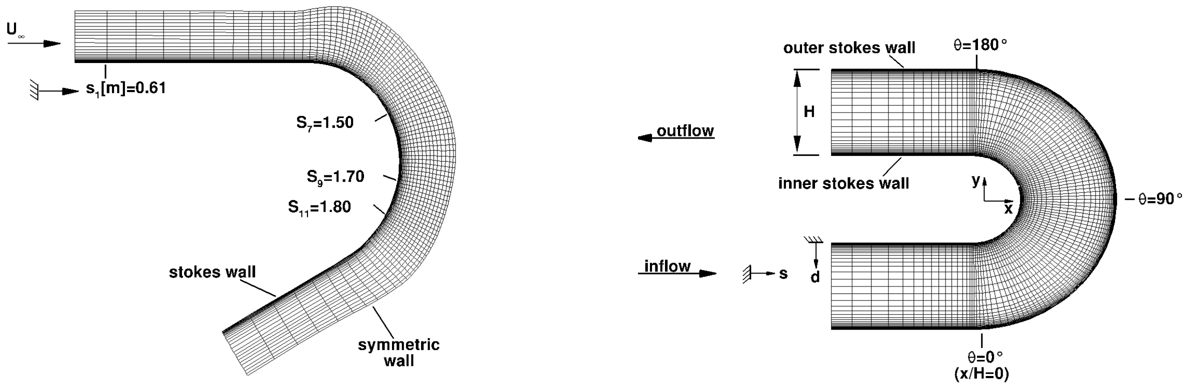

(a) Curved Bend (b) U-Duct

Figure 9: Computational Domain For Curved Bend And U-Duct

Reynolds number per metre is $1.42 \cdot 10^6$ and the Mach number at the inlet is $Ma = 0.063$. Furthermore, the velocity profile has been prescribed at the inlet, in order to meet the measurements at the position upstream of the bend ($s = 0.61m$). The U-duct of Monson and Seegmiller is also a test case where curvature dampes and amplificates the turbulence production like in a real turbomachine. The geometry of this test case is illustrated in Fig. 9 b). For the present validation, the Reynolds number of $1 \cdot 10^6$ has been set. This Reynolds number is based on a channel heights of $H = 3.81cm$ and a bulk velocity of $U_b = 31.1m/s$. Figure 10 a) and b) show again a good agreement between experiments and the numerical simulation with the new approach (VB). For more information about the numerical investigation of curved bend and U-duct the reader is refferd to Kožulović [11].

4 CONCLUSIONS

A correlation for the prescription of the turbulence length scale at inflow boundaries is provided. This correlation aims at high turbulence turbomachinery flows. Furthermore, the free stream sensitivity of the turbulence model is suppressed by a limitation of eddy

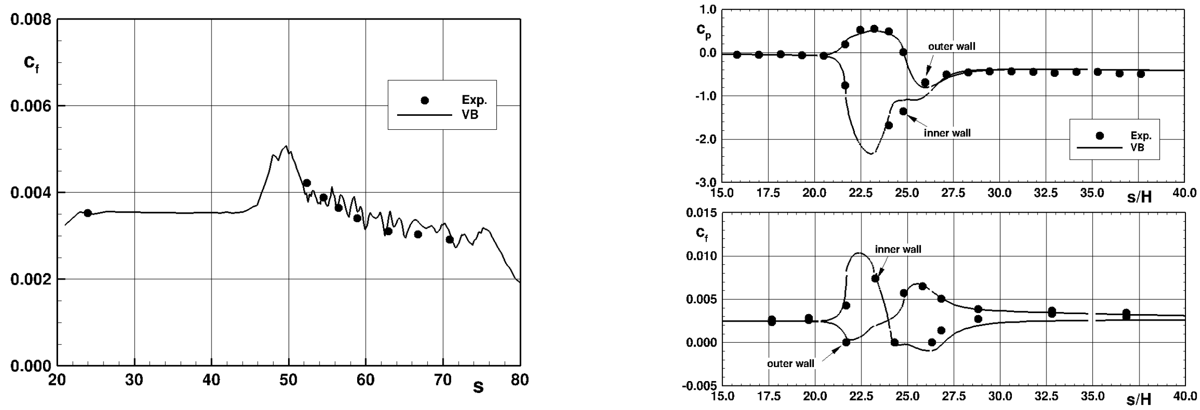

(a) Curved Bend

(b) U-Duct

Figure 10: Boundary Layer Values for Curved Bend And U-Duct

viscosity in the non-viscous regions. The method is implemented in a framework of the $k-\omega$ two-equation turbulence model and the γ-Re_θ transition model. The new approach (VB) is tested and validated at the T161 turbine cascade and generic test cases like flat plate, curved bend and U-duct. The influence of turbulence length scale at the transition location, loss coefficients, pressure distributions and turbulence quantities is evaluated. Overall, the new approach (VB) yields reasonable turbulence dissipation rates and also a very good agreement with the measurements.

ACKNOWLEDGMENT

The authors gratefully acknowledge the substantial contributions of the DLR Institute of Propulsion Thechnology and MTU Aero Engines. Prof. Dr.-Ing. Reinhard Niehuis from the University of the Armed Forces in München are thanked for providing the T161 turbine cascade hardware. Furthermore, the authors thank MTU Aero Engines for the permission to publish this work.

REFERENCES

[1] Wilcox, D. C., 2006. *Turbulence Modeling for CFD.* DCW Industries, La Canada.

[2] Langtry, R. B., and Menter, F. R., 2009. *Correlation-Based Transition Modeling for Unstructured Parallelized Compuational Fluid Dynamics Codes.* AIAA Journal, Vol. 47, No. 12.

[3] Gier, J., Franke, M., Hübner, N., and Schröder, T., 2010. *Designing Low Pressure Turbines for Optimized Airfoil Lift.* Journal of Turbomachinery, 132(2), p. 031008.

[4] Roach, P. E., and Brierley, D. H., 1990. *The influence of a turbulent free stream on zero pressure gradient transitional boundary layer development*. Tech. rep., Cambridge University Press, (Numerical simulation of unsteady flows and transition to turbulence).

[5] Monson, D. J., and Seegmiller, H. L., 1992. *An Experimental Investigation of Subsonic Flow in a Two-Dimensional U-Duct*. NASA Technical Memorandum 103931, Ames Research Center, California, July.

[6] So, R. M. C., and Mellor, G. L., 1972. *An Experimental Investigation of Turbulent Boundary Layers along Curved Surfaces*. NASA Contractor Report 1940, Princeton University, April.

[7] Bode, C., Kožulović, D., Franke, M. and Westhäuser, K., 2011. *Incorporating the Effects of Turbulence Length Scale in Turbulence and Transition Models for Turbomachinery Flows*. Proc. 60th DLRK, Paper No. DLRK-1466, Bremen (Germany).

[8] Bode, C., Aufderheide, T., Kožulović, D. and Friedrichs, J., 2014. *The Effects of Turbulence Length Scale on Turbulence and Transition Prediction in Turbomachinery Flows*. Proc. of the ASME Turbo EXPO, Paper No. ASME-GT2014-27026, Düsseldorf (Germany).

[9] Moore, J. G. and Moore, J., 1999. *Realizability in Turbulence Modelling for Turbomachinery CFD*. In ASME Paper No. 99GT-24.

[10] Kato, M., and Launder, B. E., 1993. *The Modelliing of Turbulent Flow Around Stationary and Vibrating Square Cylinders*. Proc. 9th Symp. on Turb. Shear Flow, Vol. 9, pp. 10.4.110.4.6.

[11] Kožulović, D. and Röber, T., 2006. *Modelling the Streamline Curvature Effects in Turbomachinery Flows*. Proc. of the ASME Turbo EXPO, Paper No. ASME-GT2006-90265, Barcelona (Spain).

[12] Baines, P. E., and Peterson, E. G., 1951. *An Investigation of Flow through Screens*. In ASME Paper No. 50-A-23.

[13] Durbin, P. A., 1996. *On the k-ϵ Stagnation Point Anomaly*. Int. J. Heat and Fluid Flow, 17, pp. 8990.

[14] Menter, F. R., 1994. *Two-equation eddy-viscosity turbulence models for engineering applications*. AIAA Journal, Vol. 32, No. 8, pp. 1598-1605.